Dynamics of Lattice Models of Polymer Chains near the Θ Point

James Patton Downey and Jeffrey Kovac*

Department of Chemistry, University of Tennessee, Knoxville, Tennessee 37996-1600

Received April 21, 1989; Revised Manuscript Received December 19, 1989

ABSTRACT: Dynamic Monte Carlo simulations were performed for isolated polymer chains on both simple cubic and face-centered cubic lattices with a rigorous excluded-volume constraint and a nearest-neighbor interaction, ϵ (i.e., a square well potential) between the nonbonded beads of the chain. The chains were observed to exhibit Rouse-like dynamics in the good solvent (or high-temperature) regime and for repulsive interactions. Relaxation times of the normal coordinates, τ, were fit to the scaling relations $\tau(N,k) \sim (N-1)^{\alpha_k}$ $\tau(N,k) \sim k^{-\gamma_N}$ where N is the number of beads in the chain and k is the mode number. α_k was observed to be dependent on k for the values of ϵ studied and γ_N was found to be dependent on $N-1$ as the Θ point was approached. Above the Θ point the scaling behavior for the two lattices was the same for a given value of $\mu\epsilon$, where μ is the effective coordination number (the coordination number of the lattice minus 1). For the short chains studied the Θ point was observed to be at approximately $\mu\epsilon = -1.8k_BT$. Near and below the Θ point, however, the dynamics of both models are significantly different from the Rouse prediction, probably due to the increasing lifetime of nearest-neighbor pair contacts. This observation is consistent with the concept of gel modes introduced by Brochard and de Gennes.

Introduction

One of the important developments in the study of polymer dynamics in the past 10 years or so has been the increased use of computer simulations to gain insight into some of the fundamental processes that occur when macromolecules move in solution or in the melt. Considerable effort has been expended in attempting to understand the effects of excluded volume on the chain dynamics in both dilute and concentrated systems, including studies of the validity of the reptation model. Less attention, however, has been paid to the role of the effective pair interactions in chain dynamics.

Monte Carlo computer simulations of lattice models have provided some important results concerning the dynamics of chains with excluded volume. These models are particularly convenient because the excluded-volume constraint can be rigorously included, but the model is simple enough that long chains and concentrated systems can be studied. A number of research groups have further developed the original model of Verdier and Stockmayer[1] and applied it to a variety of problems.[2]

Work in this research group has concentrated on the development of the model and the study of the effects of lattice coordination number on the chain dynamics.[3-7] Chains with constant bond lengths but without other self-interactions between the beads of the chain (e.g., excluded volume) exhibit the Rouse dynamics predicted for an ideal chain. When excluded-volume interactions are included, the dynamics agree well with the scaling theories for a Rouse-like chain, except that an unusual, and yet unexplained, dependence of the relaxation times on the mode number has been observed. Experimental results on real polymer chains at the Θ point are well described by the Rouse model of ideal phantom chains, but this behavior is a result of a cancellation of the effects of the excluded volume by the polymer–solvent interactions. This is relatively well understood for equilibrium properties of the chain, but the effects of the cancellation on the chain dynamics have not been extensively studied.

An early attempt to study the dynamics of polymer chains near the Θ point by computer simulation was made by Romiszowski and Stockmayer[8] who used a weighted multiple-occupancy model to study the effect of variable excluded volume on chain dynamics. The Romiszowski–Stockmayer model does give the proper equilibrium properties but, because of the use of multiple site occupancy, it does not maintain the dynamic excluded-volume constraint rigorously. Consequently, the Romiszowski–Stockmayer model cannot study the cancellation of the two effects. What is needed is a model in which both the excluded-volume condition and the attractive effects of the solvent are included explicitly.

Naghizadeh and Kovac,[6,7] extending the work of Crabb and Kovac,[9] developed an algorithm for cubic lattice model simulations in which the both the excluded volume and a nearest-neighbor interaction can be included. This algorithm has been used to study the relaxation of the end-to-end vector and the center-of-mass diffusion coefficient of isolated cubic lattice chains in the good solvent regime, near the Θ point, and in the collapsed chain regime. In the present paper we examine the dynamics of both simple cubic and face-centered cubic lattice chains in the good solvent and Θ regions in more detail.

In the Crabb–Naghizadeh–Kovac model beads are allowed to interact with their nonbonded nearest neighbors through a square well potential. In the present study the value of this potential has been varied over a wide range, from repulsive interactions to attractive interactions strong enough to simulate a Θ solvent. The dynamics have been studied by determining the relaxation times of the autocorrelation functions of the first three normal coordinates and of the end-to-end vector for a number of chain lengths. These relaxation times have been used to obtain scaling exponents for both the chain length and mode number dependences of the relaxation times. The relationship between static and dynamic scaling exponents has been examined.

The overall behavior of the exponents as a function of the attractive energy shows a gradual transition from good solvent to Θ solvent behavior consistent with Rouse-like dynamics. The two lattice models show essentially identical behavior as a function of $\mu\epsilon$ where μ is the lattice coordination number minus 1 and ϵ is the intersegment energy. This is the effective potential introduced by McCrackin, Mazur, and Guttman[10] in their studies of the lattice dependence of static chain properties. They showed that the equilibrium properties of various lattice models

0024-9297/90/2223-3013$02.50/0

of polymers were identical if plotted as a function of the effective potential $\mu\epsilon$.

In the Θ region and below the dynamics change significantly, although the change is less dramatic for the face-centered cubic model than for the simple cubic model. The relaxation time of the $k = 3$ mode is significantly slowed relative to the two longer wavelength modes. There are three factors that might be responsible for the change.

The first factor is the increasing segment density as the chain collapses. It has previously been shown that increased segment density will cause the two-bead crankshaft motions used in the simple cubic lattice model to be preferentially frozen out, resulting in a significant change in the chain dynamics.[11] The coil densities near the Θ point, however, are probably too small to explain the effects observed here. In addition, increasing coil density should affect all modes in the same way.

A second factor is local chain stiffness resulting in coil expansion on the short range. Curro and Schaefer have reported results of a Monte Carlo simulation in which they found that the end-to-end distances of interior chain sequences of n bonds were larger than those of free chains of the same length.[12] This observation is inconsistent with the usual blob model but is not unreasonable for the short chains used in the present study. This short-range chain expansion would result in the slowing down of the higher k modes if these modes obey the dynamic scaling hypothesis.

The third, and most likely, possibility is the dynamic affect of the increasing lifetime of pair contacts as the nearest-neighbor interaction becomes more attractive. If this lifetime becomes comparable to the relaxation time of a particular normal mode, then the behavior of that mode should be significantly affected. Clearly the $k = 3$ mode with the shortest relaxation time should show the largest effect. This idea was suggested originally by Brochard and de Gennes[13] with the picturesque name of "gel modes".

Any or all of these factors could be important for the dynamics observed here in the Θ region and below. Unfortunately, our results are unable to clearly separate the relative importance of the three mechanisms, although the gel modes seem to be the most important factor. An even more detailed analysis of both the static and dynamic properties of the chain will be necessary.

Simulation Model

For this study we used the algorithm developed by Naghizadeh and Kovac[6,7] and its extension to the face-centered cubic lattice. The computer algorithm including nearest-neighbor interactions is a straightforward modification of the models originally developed by Crabb and Kovac[9,14] and Downey, Crabb, and Kovac.[4] The elementary motions have been discussed in detail in previous articles so they will be only briefly reviewed here.

In the Crabb–Naghizadeh–Kovac simple cubic lattice model, the bonds of the chain are of fixed length. Therefore, if an interior bead is in a linear alignment with its bonded neighbors, this constraint makes motion of this bead impossible. A bead in the interior of the chain may move by a bond vector exchange with its two bonded neighbors. This is referred to as a normal bead motion. If this move is disallowed due to the excluded-volume condition, then the local conformation of the chain is analyzed and, if it is a crankshaft configuration, a crankshaft motion with the appropriate neighboring bead is attempted. This two-bead crankshaft may move to one of the two locations that lie in the plane positioned at a 90° angle to the plane in which the crankshaft was originally located. End beads are allowed to move to one of four positions that are nearest neighbors to the next-to-end bead and form a 90° angle to the end bead's original vector from the next-to-end bead.

Beads that are not bonded to one another interact by a nearest-neighbor square well potential, $V(r)$, with the property

$$V(0) = \infty \qquad V(l_o) = \epsilon \qquad V(r) = 0 \quad \text{for } r > l_o \tag{1}$$

where l_o is the distance between nearest neighbors. An attempted bead movement beings when the computer generates a random integer, J, such that $1 \le J \le N$. The bead J is then analyzed to determine whether an end bead, normal bead, or crankshaft motion will be attempted. (A linear conformation, of course, results in a termination of the attempted move.) Once the local conformation has been determined, the unnormalized probabilities P_i for each possible location to which the bead(s) may move as well as the probability of remaining at rest are calculated by the formula

$$P_i = \exp(\phi n_i) \tag{2}$$

where $\phi = -\epsilon/k_B T$ and n_i is the number of nonbonded nearest-neighbor interactions at position i for the bead(s) involved in the move. P_i is set to be zero if the excluded-volume condition is violated. The random number generator then produces a number G such that

$$0 < G \le \sum_i P_i \tag{3}$$

The beads are moved to location i if

$$\sum_{k=1}^{i-1} P_k < G \le \sum_{k=1}^{i} P_k \tag{4}$$

These transition probabilities are consistent with the principles of microscopic reversibility and detailed balancing.

For the face-centered cubic lattice model the elementary motions are described in detail in the original article by Downey, Crabb, and Kovac[4] and are only briefly reviewed here. The interior beads of the chain lie at the center of an angle formed by the bonds of the two nearest-neighbor beads. This angle may be 60°, 90°, 120°, or 180°. If the angle is 180°, no motion of the bead is possible since, in this model, the bonds are of fixed length. If the angle is 120°, the only motion possible is an in-plane, bond vector exchange. For both the 60° and 90° angle configurations there are three possible motions. One is an in-plane bond vector exchange; the other two are out-of-plane, crankshaftlike motions, which maintain the fixed bond lengths of the chain. End beads may move to any of the other 11 lattice positions that are nearest neighbors to the next-to-end bead subject, of course, to the excluded-volume constraint. The individual transition probabilities are chosen as described above.

To analyze the dynamics of the chain, the end-to-end vector, $\vec{R}(t)$, was used to compute the autocorrelation function

$$\rho_R(t) = \langle \vec{R}(t)\cdot\vec{R}(0)\rangle / \langle R^2 \rangle \tag{5}$$

The pointed brackets represent an ensemble average computed as a time average over a trajectory begun from an equilibrated chain conformation. In order to examine the internal dynamics of the chains, we used the normal

coordinates, $\vec{U}_k(t)$, given by the Rouse formula[15]

$$\vec{U}_k(t) = \sum_{j=1}^{N} [(2 - \delta_{k0})/N]^{1/2} \cos [(j - 1/2)\pi k/N] \vec{R}_j(t) \quad (6)$$

From this formula we obtain the autocorrelation functions of the normal coordinates.

$$\rho_k(t) = \langle \vec{U}_k(t) \cdot \vec{U}_k(0) \rangle / \langle U_k^2 \rangle \quad (7)$$

The ensemble averages were computed from values of $\vec{R}_j$ for each bead j sampled at time intervals corresponding roughly to a decay in the value of $\rho_1(t)$ of about 0.7%. At least 20 000 samples were taken for each run.

The relaxation times of the autocorrelation functions were found by plotting ln $\rho(t)$ vs time, where the time unit is taken to be N bead cycles. The relaxation time, τ, is the negative of the inverse of the slope of this line. For the normal coordinates, the slope was obtained by an unweighted least-squares fit over the range for which

$$0 \leq \ln \rho_k(t) \leq -1.2 \quad (8)$$

For the end-to-end vector relaxation times, the range used was

$$-0.4 \leq \ln \rho_R(t) \leq -1.2 \quad (9)$$

The values of τ and $\langle R^2 \rangle$ used in this study were the average of at least four runs. Simulations were performed for chains of 24, 36, 48, 60, and 72 beads. All simulations were performed on a Hewlett Packard 1000 Model A900 computer using FORTRAN source codes.

Results and Discussion

The scaling exponents, α_k, for the normal-coordinate relaxation times were obtained by fitting an unweighted least-squares line to a double logarithmic plot of the relaxation time, τ_k, versus the chain length, $N - 1$. These exponents correspond to the scaling relation

$$\tau_k(N) \sim (N - 1)^{\alpha_k} \quad (10)$$

The scaling exponent, α_R, for the end-to-end vector relaxation time, τ_R, was obtained similarly except, in this case, only the linear long-time region is used to calculate the relaxation time. This exponent corresponds to the scaling relation

$$\tau_R(N) \sim (N - 1)^{\alpha_R} \quad (11)$$

The values of α_k and α_R for the simple cubic lattice are listed in Table I, and the values for the face-centered cubic model are in Table II. The values for both models are plotted in Figure 1 for the different values of $\mu(\phi)$. As expected, the values of α_k decrease with increasing $\mu(\phi)$ (i.e., making the interaction more attractive). The attractive nearest-neighbor interaction offsets the expansion caused by excluded volume, and, therefore, we see the values of α_k begin to approach the value of α expected for an ideal chain (i.e., the Θ point value of $\alpha_k = 2.0$). Throughout the good solvent region we find $\alpha_1 = \alpha_R$. This is to be expected since the first normal mode dominates the long-time behavior of the end-to-end vector. As we pass the Θ point, we find $\alpha_1 > \alpha_R$.

We find, however, that the semilogarithmic plots of the end-to-end vector autocorrelation functions being to lose their linearity at long times. This is due to the fact that the relaxation times of the higher k modes are becoming larger and the decay of $\rho_R(t)$ is not being followed long enough to reach the linear long-time region. We do find, however, the semilog plots of the autocorrelation functions of the normal modes to be linear at all potentials we have studied. This indicates that the Rouse coordinates are still a good set of normal coordinates even in the dense environment of the collapsing chain. We have also calculated the cross correlations $\langle \vec{U}_k(t) \cdot \vec{U}_j(t) \rangle$ and found them to be zero. This corroborates the earlier observation that the Rouse coordinates are a good set of normal coordinates in dense polymer systems and suggests that this will remain true even for dense systems interacting through a nearest-neighbor potential.

For essentially all potentials studied with both models we find $\alpha_1 < \alpha_2 < \alpha_3$. The few exceptions are almost certainly due to statistical fluctuations. This is in general agreement with our previous Monte Carlo studies[3-5] with no potential ($\phi = 0$) in which we also found $\alpha_1 < \alpha_2 < \alpha_3$. This observation is consistent with the effects of local chain stiffness and with the observation of Curro and Schaefer who found local expansion of the chain in the good solvent region. As the Θ point is approached from above the values of all the α_k become smaller. Below the Θ point this behavior changes significantly. The values of α_1 continue to decrease for both models. α_2 for the simple cubic lattice increases slowly while in the face-centered cubic lattice it decreases slowly. The values of α_3 for the simple cubic lattice begin to increase rather sharply while, for the face-centered cubic lattice, they remain essentially constant.

This behavior is partly due to the increasing segment density in the coil interior. Increasing segment density will increase the value of the scaling exponents as was

Table I
Values of the Dynamic Scaling Exponents α_R and α_k and the Static Scaling Exponent 2ν for Various Values of the Pair Interaction Potential $\varphi = -\epsilon/k_BT$ for the Simple Cubic Lattice Model[a]

$-\epsilon/k_BT$	α_R	α_1	α_2	α_3	2ν	$\alpha_R - 2\nu$	$\alpha_1 - 2\nu$
−0.20	2.31	2.30	2.26	2.29	1.23	1.08	1.07
−0.10	2.13	2.14	2.24	2.28	1.19	1.06	0.95
0.0	2.35	2.30	2.22	2.25	1.22	1.13	1.08
0.10	2.21	2.14	2.15	2.24	1.19	1.02	0.95
0.20	2.17	2.18	2.15	2.16	1.10	1.07	1.08
0.30	2.08	2.07	2.11	2.18	1.01	1.07	1.06
0.32	2.07	2.06	2.10	2.12	1.00	1.07	1.06
0.34	2.04	2.05	2.09	2.13	0.98	1.06	1.07
0.36	1.99	1.99	2.08	2.14	0.93	1.06	1.07
0.38	1.98	2.02	2.05	2.13	0.89	1.09	1.13
0.40	1.92	2.02	2.08	2.15	0.84	1.04	1.18
0.50	1.74	1.90	2.12	2.30			

[a] These exponents are defined in eqs 10–12. In the final two columns the differences $\alpha_1 - 2\nu$ and $\alpha_R - 2\nu$ used to test the dynamic scaling hypothesis are given.

Table II
Values of the Exponents α_R and α_k for Various Values of the Pair Potential $\varphi = -\epsilon/k_BT$ for the Face-Centered Cubic Lattice Model[a]

$-\epsilon/k_BT$	α_R	α_1	α_2	α_3	2ν	$\alpha_R - 2\nu$	$\alpha_1 - 2\nu$
−0.10	2.15	2.15	2.27	2.39	1.22	0.93	0.93
−0.05	2.28	2.27	2.28	2.33	1.20	1.08	1.07
0.0	2.23	2.18	2.26	2.35	1.21	1.02	0.97
0.05	2.15	2.13	2.19	2.26	1.20	0.95	0.93
0.10	2.18	2.19	2.12	2.22	1.10	1.08	1.09
0.12	2.01	2.05	2.16	2.17	1.03	0.98	1.02
0.14	2.05	2.07	2.09	2.15	1.03	1.02	1.04
0.16	2.15	2.11	2.07	2.11	1.01	1.14	1.10
0.18	1.82	1.86	2.08	2.24	0.84	0.98	1.02
0.20	1.82	1.86	2.07	2.24	0.78	1.04	1.08
0.25	1.50	1.68	2.01	2.12			

[a] These exponents are defined in eqs 10–12. Also given are the values of the static scaling exponent 2ν and the differences $\alpha_R - 2\nu$ and $\alpha_1 - 2\nu$ used to test the dynamic scaling hypothesis.

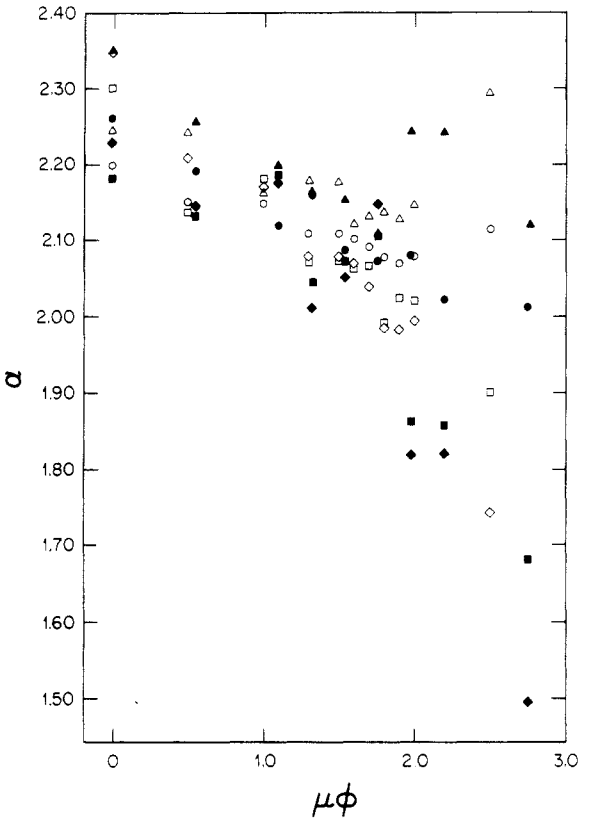

Figure 1. Plot of α_R (◇), α_1 (□), α_2 (○), and α_3 (△) plotted against $\mu\phi$. The filled symbols are for the face-centered cubic lattic. The open symbols are for the simple cubic lattice.

clearly shown by earlier work on concentrated systems. The coil densities, $N/\langle R^2\rangle^{3/2}$, near the Θ point are still rather small and, on the basis of previous results on dense system dynamics, are probably not the major factor in the increase of the scaling exponent α_3. In addition, the results on dense systems showed that increasing segment density had a similar effect on all three modes.[11,16] This is not true here. α_1 continues to decrease below the Θ point while α_3 increases or remains constant.

Another, probably more important, factor is the effect of the attractive potential. Each nearest-neighbor contact will have a finite mean lifetime determined by the strength of the interaction compared to the thermal energy. If that lifetime is long compared to the relaxation time of the motion, then one should see a slowing of the relaxation. Clearly, the higher k modes will be more strongly effected by this mechanism than the long wavelength modes. This is the physical origin of the gel modes introduced by Brochard and de Gennes.[13] What we observe here might be an indication of these gel modes, but a more detailed study of the chain motion would be required to clearly separate the effects of chain stiffness and nearest-neighbor attractions.

The mean-square end-to-end distances measured for the various potentials were fit to the scaling relation

$$\langle R^2\rangle \sim (N-1)^{2\nu} \tag{12}$$

The values of 2ν are listed in Tables I and II and plotted in Figure 2 as a function of the reduced effective potential, $\mu\phi$. Experimental measurements, scaling theories, and static and dynamic Monte Carlo methods give values of ν to be about 0.6 for a good solvent. The values obtained are consistent with previous results. In Figure 2 it can be seen that 2ν varies smoothly with $\mu\phi$. The values of 2ν obtained below the Θ point are of debatable merit since we found the lines from which they are drawn

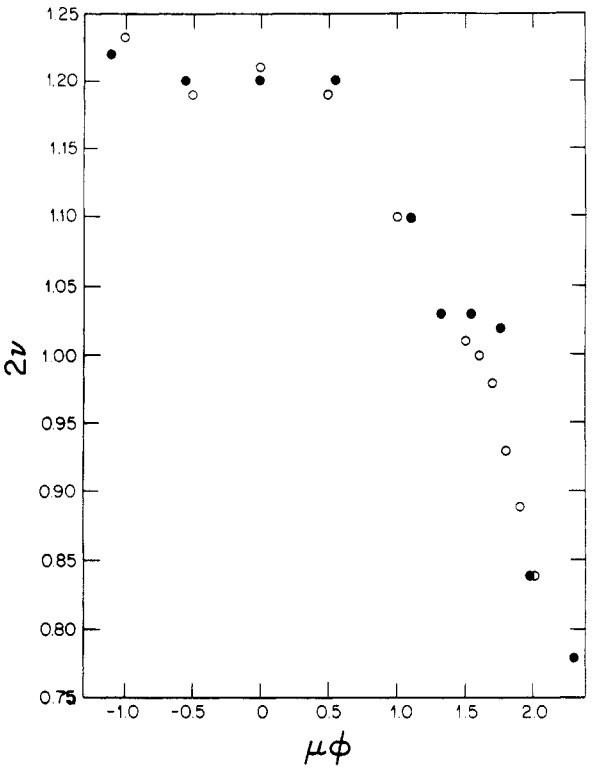

Figure 2. Plot of the static scaling exponent, 2ν, versus $\mu\phi$ for the face-centered cubic (●) and simple cubic lattice (○).

begin to lose their linearity as we pass the Θ point. This latter observation is consistent with the previous results of Naghizadeh and Kovac who found that the $\langle R^2\rangle$ vs N plots became curved in the collapsed chain region, eventually going over to the behavior expected for a collapsed coil.

The relaxation times of the end-to-end vector and the first normal mode are fit by the relation

$$\tau \sim \langle R^2\rangle(N-1) \sim (N-1)^{2\nu+1} \sim \langle R^2\rangle^{1+1/2\nu} \tag{13}$$

The exponent $1 + 1/2\nu$ is usually referred to as the dynamic scaling exponent and is denoted as z. We have previously defined $2\nu + 1 = \alpha$. It had been shown by renormalization group techniques that chains with excluded volume and Rouse-like dynamics have the scaling property $z = 1 + 1/2\nu$; i.e. $\alpha = 2\nu + 1$.[9] This is referred to as the dynamic scaling result.

In this study we found the values of 2ν using static measurements and the values of α from dynamic measurements. In Tables I and II, we list $\alpha_1 - 2\nu$ and $\alpha_R - 2\nu$ for potentials above the Θ point, i.e., $\phi < 0.34$ for the simple cubic lattice model and $\phi < 0.17$ for the face-centered cubic lattice model. We find these differences to be in good agreement with the dynamic scaling result of $\alpha - 2\nu = 1.0$. For the simple cubic lattice model below the Θ point $\alpha_1 - 2\nu$ increases, but $\alpha_R - 2\nu$ remains relatively constant. While it is interesting that α_R and 2ν remain interdependent as we enter the poor solvent regime, our lack of confidence in the values of α_R and 2ν in this regime cause us to distrust putting much emphasis on this result.

We have also fit the relaxation times of the normal coordinates to the scaling relation

$$\tau(N,k) \sim k^{-\gamma_N} \tag{14}$$

The values obtained for γ_N are listed in Tables III (simple cubic) and IV (face-centered cubic) and plotted in Figure 3 as a function of $\mu\phi$. The values of γ_N decrease

Table III
Values of the Scaling Exponent γ_N for Various Values of the Pair Interaction Potential $\varphi = -\epsilon/k_BT$ for the Simple Cubic Lattice Model[a]

$-\epsilon/k_BT$	γ_{24}	γ_{36}	γ_{48}	γ_{60}	γ_{72}
−0.20	2.23	2.26	2.29	2.27	2.24
−0.10	2.30	2.20	2.25	2.15	2.14
0.0	2.10	2.09	2.06	2.10	2.20
0.10	2.17	2.15	2.09	2.10	2.13
0.20	1.91	1.99	1.96	2.01	2.09
0.30	1.91	1.89	1.80	1.78	1.79
0.32	1.80	1.84	1.83	1.79	1.74
0.34	1.80	1.76	1.73	1.73	1.73
0.36	1.78	1.71	1.66	1.63	1.64
0.38	1.73	1.64	1.65	1.64	1.61
0.40	1.71	1.67	1.63	1.55	1.53
0.50	1.41	1.40	1.17	1.19	1.00

[a] The exponent is defined in eq 14.

Table IV
Values of the Exponents γ_N for Various Values of the Pair Interaction Potential $\varphi = -\epsilon/k_BT$ for the Face-Centered Cubic Lattice Model[a]

$-\epsilon/k_BT$	γ_{24}	γ_{36}	γ_{48}	γ_{60}	γ_{72}
−0.10	2.36	2.18	2.21	2.12	2.10
−0.05	2.19	2.02	2.11	2.20	2.13
0.0	2.23	2.24	2.09	2.11	2.08
0.05	2.19	2.02	2.01	2.13	2.05
0.10	2.06	1.96	1.92	1.93	2.09
0.12	2.02	2.00	1.93	2.00	1.83
0.14	1.92	1.87	1.84	1.83	1.86
0.16	1.82	1.71	1.84	1.81	1.78
0.18	1.86	1.90	1.61	1.62	1.51
0.20	1.75	1.76	1.52	1.52	1.37
0.25	1.46	1.35	1.29	1.03	1.04

[a] This exponent is defined in eq 14.

with decreasing ϕ, and, at least near the Θ region and below, γ_N decreases for increasing N. Decreasing values of γ_N indicate that the shorter range motions are becoming more inhibited relative to the longer range motions. This is consistent with the hypothesis that the relaxation time of nearest-neighbor contacts is exerting an effect on the dynamics in the Θ region. This effect becomes greater for larger N and for larger (more attractive) values of ϕ. The decrease in γ_N is probably not a density effect since it has been shown that γ_N is only weakly dependent on density and at very high densities γ_N approaches the Rouse value of 2.0.[11,16] Unexpectedly low values of γ_N could be explained by the observation of Curro and Schaefer, but the internal chain expansion they observed seemed to disappear just below the Θ point. Since longer chains are more flexible and will have more nearest-neighbor contacts this observation is consistent with the existence of gel modes in the Θ region.

The difference between the dynamics of the two lattice models below the Θ point is probably due to the differences in the elementary motions used in the two models. The simple cubic lattice model requires the use of the two-bead, three-bond crankshaft motion. This longer range elementary motion will be more strongly effected by both the increasing segment density and the increased lifetime of the pair contacts than a single bead motion. Since the face-centered cubic lattice model uses only single bead motions, it should be effected differently by the increasing attraction. The difference in the effect of increasing concentration on the two different models was seen in the work of Crabb, Hoffman, Dial, and Kovac.[16]

The Θ point is defined as the point at which the chain's attractive interactions cause it to behave as an ideal chain. However, there is no reason to believe that all the properties of an ideal chain will occur at the same value of ϕ.

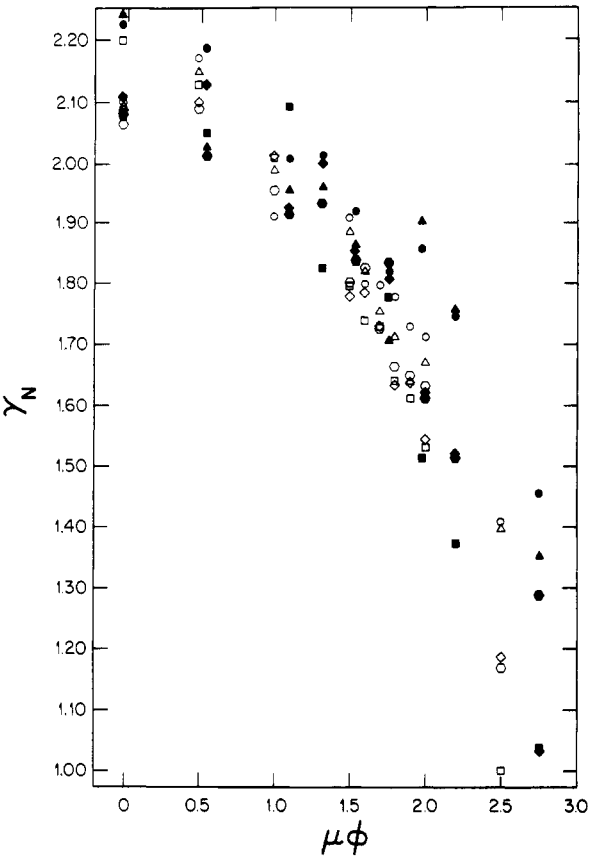

Figure 3. Plot of γ_{24} (○), γ_{36} (△), γ_{48} (○), γ_{60} (◇), and γ_{72} (□) versus $\mu\phi$. The filled symbols are for the face-centered cubic lattice. The open symbols are for the simple cubic lattice.

Therefore, some authors refer to a Θ region in which various characteristics of the Θ point are satisfied. In our study we have located the Θ point using a variety of different parameters.

For an ideal chain the value of 2ν should be 1.0. From Table I, we find this occurs in the region of $0.34 < \phi < 0.36$ for the simple cubic lattice model. For the face-centered cubic lattice the Θ point is at approximately $\phi = 0.17$. These correspond to essentially the same value of the effective potential, $\mu\phi = 1.8$. The effective potential corresponding to the Θ point is slightly smaller for the simple cubic lattice than for the face-centered cubic lattice. This is probably due to the larger persistence length of the simple cubic lattice chains. This chain stiffness will effect the position of the Θ point of short chains, but the difference should disappear as $N \to \infty$. The exponents α_1 and α_R should both be 2.0 at the Θ point. Table I shows that $\alpha_1 = 2.0$ in the range $0.34 < \phi < 0.36$, while $\alpha_R = 2.0$ in the range $0.32 < \phi < 0.34$ for the simple cubic lattice. For the face-centered cubic lattice the region at which these two exponents become equal to 2.0 is the same and is centered at $\phi = 0.17$.

As a final measure of the Θ point we have plotted $\langle R^2 \rangle / (N-1)$ vs ϕ in Figures 4 (simple cubic) and 5 (face-centered cubic). From the formula of Domb and Fisher[17] we expect this ratio to have a value of 1.5 for a simple cubic lattice and 1.2 for the face-centered cubic lattice at the Θ point. From Figures 4 and 5 it can be seen that this occurs at approximately $\phi = 0.34$ for the simple cubic lattice and $\phi = 0.16$ for the face-centered cubic lattice. Within the limits of our study this measure of the Θ point does not show an appreciable dependence on the chain length.

It is interesting that the value of γ_N reaches its ideal chain value of 2.0 at a much larger value of ϕ than the

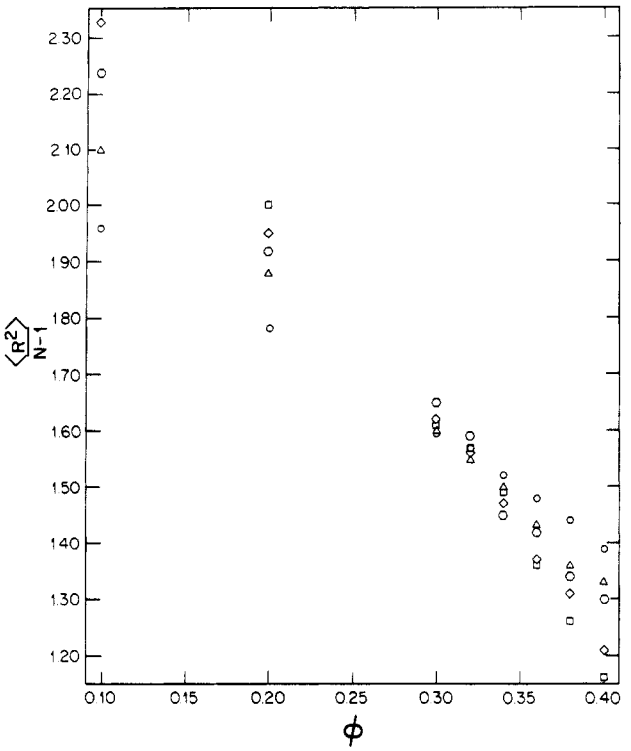

Figure 4. Plot of the reduced mean-square end-to-end distance $\langle R^2 \rangle/(N-1)$ versus the potential ϕ: $N = 24$ (○), $N = 36$ (△), $N = 48$ (○), $N = 60$ (▽), $N = 72$ (□).

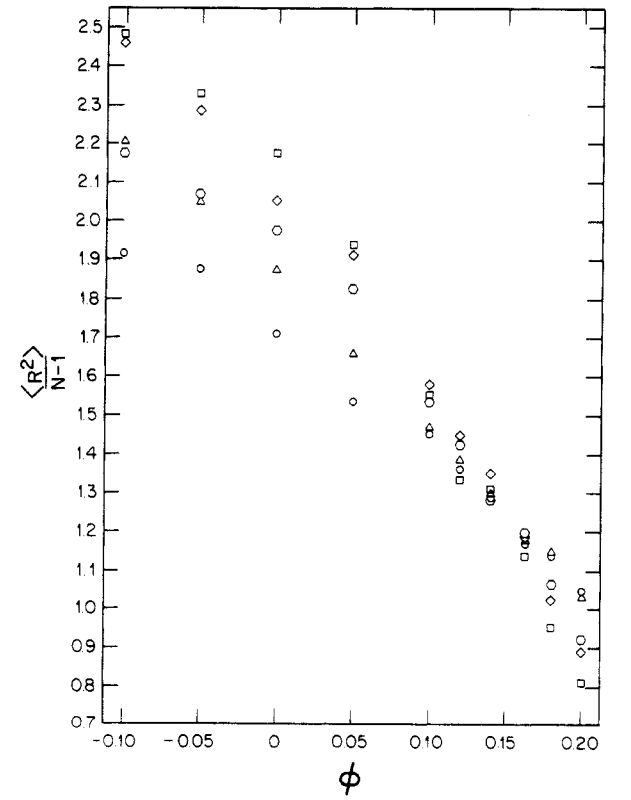

Figure 5. Plot of $\langle R^2 \rangle/(N-1)$ against ϕ: $N = 24$ (○), $N = 35$ (△), $N = 48$ (○), $N = 60$ (◇), $N = 72$ (□).

other three parameters and then continues to decrease as the attraction increases. At the Θ point γ_N is smaller than the ideal chain value. As suggested above this seems to be an indication that the finite lifetime of nearest-neighbor contacts is influencing the dynamics in the Θ region. To show graphically the way in which the values of α_k and γ_N vary as a function of the attractive energy, we have plotted α_k versus the long-chain value of γ (the

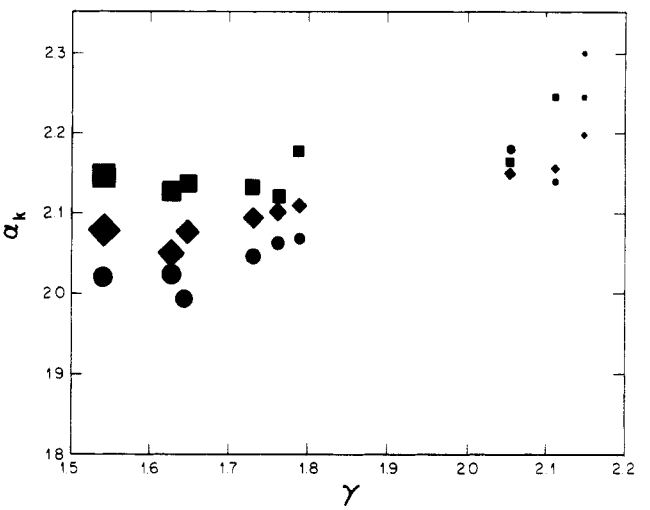

Figure 6. Plot of the exponent α_k versus the long-chain value of γ_N for different attractive energies. The long-chain value of γ_N is the average of γ_{60} and γ_{72}. The increasingly large symbols indicate increasingly large ϕ. Values of ϕ are 0.0, 0.10, 0.20, 0.30, 0.32, 0.34, 0.36, and 0.40. The three different values of α_k are designated: α_1 (○), α_2 (◇), and α_3 (□).

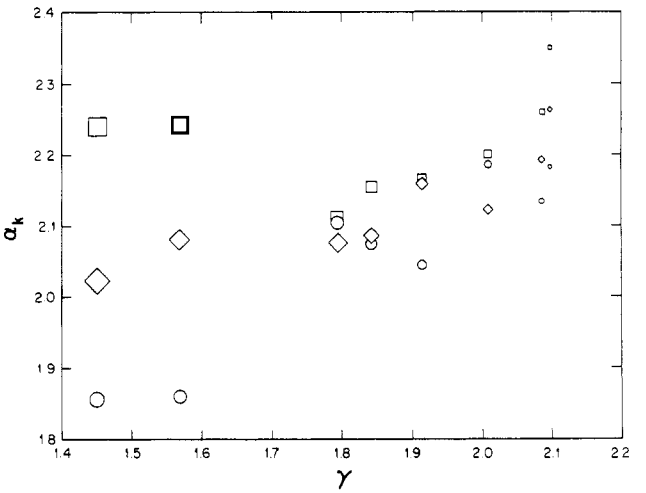

Figure 7. Plot of α_k against the long-chain value of γ_N for different attractive energies. The long-chain value of γ_N is the average of γ_{60} and γ_{72}. The increasingly large symbols indicate increasingly large values of ϕ. Values of ϕ are 0.0, 0.05, 0.10, 0.12, 0.14, 0.16, 0.18, and 0.20. Symbols are for α_1 (○), α_2 (◇), and α_3 (□).

average of the values for $N = 60$ and $N = 72$) for a number of values of ϕ in Figures 6 (simple cubic) and 7 (face-centered cubic). These values of α_k and γ correspond to a compact Rouse-like formula for the relaxation times of the form

$$\tau_k(N) = A_k(N-1)^{\alpha_k}/k^{\gamma} \qquad (15)$$

where A_k is a proportionality constant, which is indicative of the absolute time scale of the relaxation. In Figures 6 and 7 the value of the attractive energy is suggested by the size of the point. The larger the symbol the smaller (more attractive) the energy. The figure shows clearly that the ideal Rouse spectrum is never achieved by these lattice model chains. It would be interesting to see if the inclusion of the hydrodynamic interaction modified the spectrum in such a way as to produce completely Rouse-like behavior at the Θ point.

As another measure of the dynamics we have calculated the long-chain value of the parameter A_k, defined in eq 15, as a function of the interaction energy. The averages of the values of A_k for chain lengths 48, 60, and

Table V
Values of the Constant A_k Defined in Equation 15 for Various Values of the Pair Interaction Potential $\varphi = -\epsilon/k_BT$ for the Simple Cubic Lattice Model

$-\epsilon/k_BT$	A_1	A_2	A_3
-0.20	0.243	0.283	0.253
-0.10	0.404	0.295	0.230
0.0	0.195	0.277	0.250
0.10	0.340	0.332	0.229
0.20	0.255	0.303	0.282
0.30	0.351	0.285	0.219
0.32	0.342	0.297	0.262
0.34	0.359	0.303	0.252
0.36	0.424	0.298	0.233
0.38	0.377	0.334	0.246
0.40	0.369	0.283	0.213
0.50	0.490	0.214	0.0951

Table VI
Values of Constant A_k Defined in Equation 14 for Various Values of the Pair Interaction Potential for the Face-Centered Cubic Lattice Model

$-\epsilon/k_BT$	A_1	A_2	A_3
-0.10	0.476	0.293	0.173
-0.05	0.262	0.271	0.209
0.0	0.340	0.245	0.171
0.05	0.383	0.304	0.235
0.10	0.302	0.344	0.232
0.12	0.427	0.278	0.260
0.14	0.349	0.330	0.252
0.16	0.296	0.345	0.288
0.18	0.658	0.275	0.138
0.20	0.627	0.318	0.127
0.25	1.237	0.235	0.154

72 are listed in Tables V and VI. The value of A_k is a measure of the absolute time scale of the relaxation. Although there is a lot of statistical scatter, the values of A_k are, at most, weakly dependent on k. The value of A_3 is smaller than either A_1 or A_2, but all three values are relatively independent of the potential except for the most attractive values of ϕ, which are deep in the collapse region. The major effect of the attractive potential on the dynamics seems to be contained in the two scaling exponents α_k and γ_N.

As a final note, we have also performed simulations for repulsive values of the pair potential, and the results for the scaling exponents are included in the Tables. The motivation for studying these cases was to see if this simple model could be used to represent the behavior of stiff chains. We do not see an expansion of the chain or a significant effect of the dynamics for the potentials studied for either model. These results suggest that this is not an effective way to simulate extended chains. A more effective, but more complicated, way of introducing stiffness would be through the introduction of a bond–bond potential.

Conclusion

At potentials above the Θ point, both models exhibit Rouse-like dynamics. For a given value of the effective potential, $\mu\phi$, the static and dynamic scaling exponents have identical values for both the simple cubic and face-centered cubic lattices. The results of this study indicate that for swollen chains our results are not model or lattice dependent. These observations are an encouraging indication that simulations may be applied to more complex problems involving isolated swollen polymers without fera of lattice and model dependencies.

The dynamics of the two lattices appear to be quite different for collapsed chains. We believe that the reason for this is the freezing-out of the two-bead crankshaft motions in the simple cubic lattice once the chain collapses. There are several ways of testing this hypothesis. One is to study the dynamics of a body-centered cubic lattice model, which uses only one-bead elementary motions but has a different lattice coordination number. The second method is to compute the lifetimes of the pair contacts in the two models and compare them to each other and to the relaxation times of the various normal modes. We plan to report results of these investigations in future publications.

Acknowledgment is made to the U.S. Department of Energy, Office of Basic Energy Sciences, Division of Materials Sciences, and to the donors of the Petroleum Research Fund, administered by the American Chemical Society, for financial support of this work.

References and Notes

(1) Verdier, P. H.; Stockmayer, W. H. *J. Chem. Phys.* **1962**, *36*, 227.
(2) Most of this work is comprehensively reviewed in: Kremer, K.; Binder, K. *Comput. Phys. Rep.* **1988**, *7*, 259.
(3) Dial, M.; Crabb, K. S.; Crabb, C. C.; Kovac, J. *Macromolecules* **1985**, *18*, 2215.
(4) Downey, J. P.; Crabb, C. C.; Kovac, J. *Macromolecules* **1986**, *19*, 2202.
(5) Downey, J. P.; Kovac, J. *Macromolecules* **1987**, *20*, 1357.
(6) Naghizadeh, J.; Kovac, J. *Phys. Rev. B* **1986**, *34*, 1984.
(7) Naghizadeh, J.; Kovac, J. *Phys. Rev. Lett.* **1987**, *59*, 1710.
(8) Romiszowski, P.; Stockmayer, W. H. *J. Chem. Phys.* **1984**, *80*, 485.
(9) Crabb, C. C. Ph.D. Thesis, University of Tennessee, 1984.
(10) McCrackin, F. L.; Mazur, J.; Guttman, C. M. *Macromolecules* **1973**, *6*, 859.
(11) Crabb, C. C.; Kovac, J. *Macromolecules* **1985**, *18*, 1430.
(12) Curro, J. G.; Schaefer, D. W. *Macromolecules* **1980**, *13*, 1199.
(13) Brochard, F.; de Gennes, P.-G. *Macromolecules* **1977**, *10*, 1157.
(14) Gurler, M. T.; Crabb, C. C.; Dahlin, D. M.; Kovac, J. *Macromolecules* **1985**, *16*, 398.
(15) Verdier, P. H. *J. Chem. Phys.* **1966**, *45*, 2118.
(16) Crabb, C. C.; Hoffman, D. F., Jr.; Dial, M.; Kovac, J. *Macromolecules* **1988**, *18*, 2230.
(17) Domb, C.; Fisher, M. E. *Proc. Cambridge Philos. Soc.* **1958**, *54*, 48.